Estuaries and Coasts Vol. 30, No. 1, p. 102–112 February 2007

Wind-driven Sediment Suspension Controls Light Availability in a Shallow Coastal Lagoon

S. E. LAWSON[1,*], P. L. WIBERG[1], K. J. MCGLATHERY[1], and D. C. FUGATE[2,†]

[1] *Department of Environmental Sciences, University of Virginia, P. O. Box 400123, Charlottesville, Virginia 22904-4123*

[2] *Department of Physical Science, Virginia Institute of Marine Science, P. O. Box 1346, Gloucester Point, Virginia 23062*

ABSTRACT: Light availability is critically important for primary productivity in coastal systems, yet current research approaches may not be adequate in shallow coastal lagoons. Light attenuation in these systems is typically dominated by suspended sediment, while light attenuation in deeper estuaries is often dominated by phytoplankton. This difference in controls on light attenuation suggests that physical processes may exert a greater influence on light availability in coastal lagoons than in deeper estuaries. Light availability in Hog Island Bay, a shallow coastal lagoon on the eastern shore of Virginia, was determined for a summer and late fall time period with different wind conditions. We combined field measurements and a process-based modeling approach that predicts sediment suspension and light availability from waves and currents to examine both the variability and drivers of light attenuation. Total suspended solids was the only significant predictor of light attenuation in Hog Island Bay. Waves and currents in Hog Island Bay responded strongly to wind forcing, with bottom stresses from wind driven waves dominant for 60% of the modeled area for the late fall period and 24% of the modeled area for the summer period. Higher wind speeds in late fall than in summer caused greater sediment suspension (41 and 3 mg l^{-1} average, respectively) and lower average (spatial and temporal) downwelling light availability (32% and 55%, respectively). Because of the episodic nature of wind events and the spatially variable nature of sediment suspension, conventional methods of examining light availability, such as fair-weather monitoring or single in situ recorders, do not adequately represent light conditions for benthic plants.

Introduction

Although light availability is widely recognized as a key control on primary productivity in shallow aquatic systems (e.g., Duarte 1991; Kenworthy and Fonseca 1996; Moore and Wetzel 2000), the current approaches to understanding light availability, fair weather monitoring and in situ recorders, are inadequate for shallow coastal lagoons. Research on light availability in coastal systems is guided by a conceptual model that describes an increase in nutrient availability leading to an increase in pelagic primary productivity reducing light availability for benthic plants (Cloern 2001). This conceptual model is based on deep, river-fed estuaries such as the Chesapeake Bay and has led to the development of accurate, predictive numerical models, such as CE-QUAL-ICM (Cerco and Cole 1993), but these models may not be appropriate for shallow coastal lagoons.

Shallow coastal lagoons, sometimes called coastal bays, exist globally on all continents except Antarctica and have average depths of 2–5 m. This shallow depth and the lack of riverine inflow in most coastal lagoons make these systems fundamentally different from deeper estuaries. Coastal lagoons have high sediment surface area to water volume ratios, frequent wave resuspension of sediments, and low pelagic and high benthic primary productivity because most of the sediment surface is in the photic zone (Sand-Jensen and Borum 1991). These features suggest that sediment resuspension, not increased pelagic productivity, may be the dominant control on light availability in shallow coastal lagoons. Previous studies in both the Indian River Lagoon (Gallegos and Kenworthy 1996) and the Lagoon of Venice (Zharova et al. 2001) have shown suspended sediment to control light availability in these similar systems.

Accurate modeling of light availability is an important goal for successful management of coastal ecosystems, but most available models do not satisfactorily represent the physical processes that control sediment suspension and possibly light attenuation in coastal lagoons. Van Duin et al. (2001) reviewed efforts to model light attenuation in shallow water bodies and concluded that modeling light availability based on a few sites was helpful in identifying controls on light attenuation, but not adequate to depict light availability for submerged aquatic vegetation. Most of the studies reviewed were based on empirical equations relating factors

* Corresponding author; tele: 434/924-7129; fax: 434/982-2137; e-mail: sel7b@virginia.edu

† Current address: Department of Marine and Ecological Sciences, Florida Gulf Coast University, 10501 FGCU Boulevard, South Fort Myers, Florida 33965

such as wind speed and light attenuation (Van Duin et al. 2001). These empirical equations must be fit for every site and are dependent on factors such as water depth and wind fetch. Zharova et al. (2001) developed a model that accurately represented light attenuation at a single site in Venice Lagoon, but the empirical treatment of sediment suspension means that the model must be recalibrated for other locations in the lagoon. Cerco and Cole (1993, 1994) combined a water quality model and a hydrodynamic model for the Chesapeake Bay, but the model did not include sediment resuspension and would not be appropriate for shallow coastal lagoons. Blom et al. (1992, 1994) studied light attenuation in shallow Dutch lakes by combining a two-dimensional sediment suspension model (STRESS-2d), which accounts for differential transport of sediment fractions, with a light attenuation model (CLEAR) to examine the temporal and spatial patterns of light attenuation in Lake Marken (Blom et al. 1992, 1994; Van Duin et al 1992). These studies examined the role of wind forcing in light attenuation, but did not include the effects of tides.

The current study is designed to determine if a combined sediment suspension and light attenuation model is a valid, practical, and preferable way to consider light availability in shallow coastal lagoons, where tides and wind-driven forces may be important. The use of a sediment suspension model to predict light availability reflects the importance of suspended sediment and accounts for the temporal and spatial variability of this component. This approach should overcome the limitations of empirical models and incorporate the processes (currents and tides) likely controlling light availability. The model results are then viewed in the context of efforts to restore seagrass to the lagoon.

Study Site

Hog Island Bay is a shallow embayment in the Virginia Coast Reserve Long Term Ecological Research (VCR/LTER) site on the Atlantic side of the Delmarva Peninsula (Fig. 1). Much of the lagoon is bordered by *Spartina alterniflora* marshes both on the mainland and the barrier islands. The bathymetry of the area is dominated by the Machipongo Channel, which runs roughly north-south and exits the lagoon between Hog and Cobb Islands. The channel is surrounded by subtidal flats and a few intertidal relic oyster reefs, with 50% of the bay less than 1 m deep at mean low water (Oertel 2001). Hog Island Bay has no significant source of freshwater input and the tidal range is approximately 1 m. Sediment grain size decreases from fine sand to fine silt from the inlet to the mainland creeks with an average grain

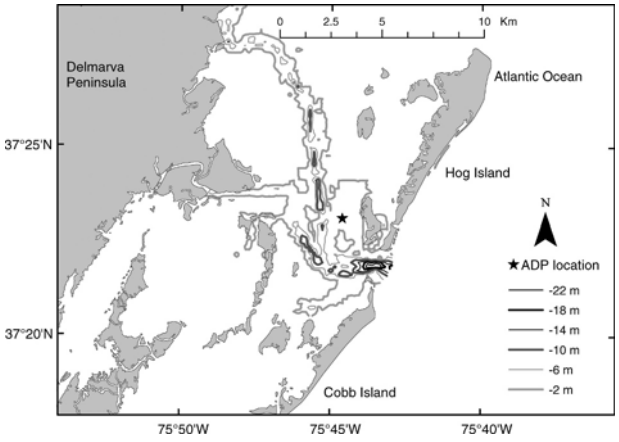

Fig. 1. Map of study site. Hog Island Bay is located on the Delmarva Peninsula and has an average depth of about 1 m. Depth contours are labeled in meters with mean sea level as zero and elevation positive up. Machipongo Channel runs roughly north-south and leaves the bay between Hog and Cobb Islands. The location of the ADP deployment is marked with a star.

size of 74 microns for the lagoon (Lawson 2004). The dominant storms in this area are nor'easters that occur from October to April. Beginning in the 1930s, Hog Island Bay, as well as lagoons to the north and south, has undergone a major state change from a seagrass-dominated (*Zostera marina*) system to an algae-dominated (macroalgae *Ulva lactuca* and *Gracilaria vermiculophylla* and benthic microalgae) system (McGlathery et al. 2001). Seagrasses are currently being restored in the coastal bays of the VCR/LTER (Orth et al. 2006).

Approach

Overview

This project examined sediment suspension and light attenuation through a combination of fieldwork and modeling. The fieldwork consisted of measurements of light availability, suspended sediment, velocity profiles, and sediment bed characteristics in Hog Island Bay. The modeling portion consisted of a sediment suspension model and an empirical equation to represent light attenuation. The shear stresses used to determine suspended sediment concentration were calculated by combining a two-dimensional finite element hydrodynamic model, Bellamy, (Ip et al. 1998) and the SWAN (Simulating Waves Nearshore) wave model (Booij et al. 1999; Ris et al. 1999). Both Bellamy and SWAN were forced with wind data from the National Oceanic and Atmospheric Administration (NOAA) Center for Operational Oceanographic Products and Services (CO-OPS) tower in Kiptopeke, Virginia (36 km from Hog Island Bay), and compared with acoustic Doppler profiler (ADP) measurements of

currents and waves at a site in Hog Island Bay during late fall. The Bellamy model was applied to Hog Island Bay by Fugate et al. (2006) to determine spatially-variable water residence times and later applied to the current study. Two time periods were modeled: late fall (19 November to 14 December 2002) and summer (7–25 August 2002).

Grid Preparation

The model area was 17 by 22 km, consisting of 9,350 200-m by 200-m grid cells (3,082 active cells). Sediment grain size was determined by a combination of wet sieving (sands) and analysis on a Sedigraph 5100 Particle Size Analyzer (muds) of triplicate samples from 82 locations in Hog Island Bay. Bathymetric data, collected in 1999–2000 using Trimble 4,000SE GPS Receivers, the Trimble NavBeacon XL, the Innerspace Digital Depth Sounder (Model 448), and the Innerspace DataLog with Guidance Software, was available from the VCR/LTER (Oertel et al. 2000, Fig. 1). Inverse distance weighted interpolation in the GRID module of ArcINFO was used to create grid surfaces for bathymetry, sediment characteristics, and Bellamy model results (water depth and velocity). The SWAN model was run using the water elevation and bathymetry grids.

Light Attenuation

Four water column components are commonly considered to attenuate light: particulate inorganic matter (PIM), particulate organic matter (POM), phytoplankton (chl *a*), and gilvin (g_{440}). An empirical relationship between these components and downwelling light attenuation (K_d) in the photosynthetically active range (400–700 nm) was developed for Hog Island Bay. Triplicate light readings, using a paired array of Li-Cor 4 pi sensors (one just below the surface and one at 1 m below), and 0.5–l water samples at 0.5 m below the surface were taken concurrently on 30 October 2003, at 16 points in Hog Island Bay. The water samples were analyzed for PIM (measured by filtration onto preweighed, precombusted Whatmann GF/F filters with a nominal particle retention size of 0.7 μm), POM (by combustion of filters used for PIM), chl *a* (measured on a spectroflourometer after 0.45 DMSO, 0.45 acetone, 0.10 deionized water, 0.001 DEA extraction), and gilvin (measured as the absorption of a filtered sample at 440 nm following Gallegos 2001). An empirical equation was generated using multiple linear regression in SAS v 8.2.

ADP Deployment

A Sontek ADP was deployed in Hog Island Bay from 17 November 2002 to 23 January 2003 and 28 April to 2 July 2004 (Fig. 1). Average water depth at the ADP site was 1.8 m. The deployment period overlapped the model run from 19 November to 14 December 2002 (the late fall run). The ADP, configured with a 0.2 m blanking distance and 0.2 m cells, measured velocity profiles, signal return strength, pressure, and standard deviation of pressure every 30 min. Suspended sediment concentration is related to the square of the signal return strength, assuming sediment and water properties are constant (Holdaway et al. 1999; Betteridge et al. 2002). A relationship between ADP backscatter signal strength and suspended sediment concentration was developed during the second ADP deployment in spring-summer 2004 (28 April to 2 July). Five replicate water samples were taken every 30 min for a total of 19 sampling events on 2 d using a horizontal Van-Dorn style bottle to sample suspended sediment concentration at the depth of the lowest bin of recorded signal amplitude on the ADP (0.84 m above the bottom).

Currents and Current Shear Stress

The Bellamy model was used to examine changes in water level and depth-averaged velocities from tide and wind-driven currents. In addition to wind data, the hydrodynamic model was forced by measured tidal elevations from NOAA stations at Wachapreague and Kiptopeke, Virginia, at the northern and southern end of the modeled area, respectively. The model was run with 300 time steps per tidal cycle, allowing 6 tidal cycles for equilibration before output was saved (Fugate et al. 2006). The non-linear system of governing equations of the model is solved iteratively at each time step. A cell is defined to be in a shallow water state when the total depth of the water column, H, plus the surface elevation relative to mean sea level, ζ, is less than 0.5 m. For shallow water cells the pressure gradient and bottom surface stress are balanced, while in deeper channels ($H + \zeta > 0.5$ m), local acceleration is added to the momentum balance. The Bellamy model solves the numerical problem of wetting and drying of intertidal cells by allowing water to continue to flow through a porous sublayer after the element becomes dry.

The model was run for the two time periods (late fall and summer) with wind forcing and for the summer time period without wind forcing. Because the model is forced with measured water levels, the effects of winds on currents cannot be fully removed, but wind effects beyond measured alterations of water level were not considered in this no wind run.

The Bellamy model produced vertically averaged velocities for each cell in the model area. Shear stresses ($\tau_{bCURRENT}$) were calculated from these

velocities using a drag coefficient (C_d) as

$$\tau_{bCURRENT} = C_d \rho U_{av}^2 \quad (1)$$

with the drag coefficient calculated from a Manning's roughness coefficient (n) as

$$C_d = \frac{gn^2}{h^{1/3}} \quad (2)$$

and the roughness coefficient calculated as

$$n = \left[\frac{2\sqrt{8g}}{h^{1/6}}\log_{10}\left(\frac{h}{D_{84}}\right) + 1\right]^{-1} \quad (3)$$

(Hornberger et al. 1998), where U_{av} is average velocity, ρ is the density of water, h is water depth, g is gravitational acceleration, and D_{84} is the grain diameter for which 84% of the sediment is smaller.

Waves and Wave Generated Shear Stress

SWAN was used to determine significant wave height (H_{sig}), wavelength (L), and wave period (T) using water levels from Bellamy and wind data from Kiptopeke. SWAN includes wave shoaling and wind-wave generation and has been shown to accurately represent waves in back barrier systems (Ris et al. 1999). For this study, SWAN was run using the default bottom friction and triad wave interactions. The hydrodynamic model output occurred on 49.82-min time steps, not the 50-min time steps used in SWAN, which resulted in a time offset of 2:20 h at the end of the November model run, the longer model run.

Wave generated shear stresses (τ_{bWAVE}) at the lagoon bottom were determined from values of H_{sig}, L, and T calculated from SWAN, with wave stress calculated as

$$\tau_{bWAVE} = \rho(f/2)\left(U_b^2\right). \quad (4)$$

The bottom wave orbital velocity (U_b) was calculated as

$$U_b = \frac{H_{sig}\pi}{T\sinh(2\pi h/L)} \quad (5)$$

The friction factor (f) was calculated based on the wave amplitude (a_b) and roughness length (k_s taken to be $3D_{84}$) as:

$$f = 0.04(a_b/k_s)^{-1/4} \quad \text{for } a_b/k_s \geq 100 \quad (6a)$$

$$f = 0.4(a_b/k_s)^{-3/4} \quad \text{for } 10 < a_b/k_s < 100 \quad (6b)$$

$$f = 0.071\left((0.4)10^{-3/4}\right) \quad \text{for } a_b/k_s < 10 \quad (6c)$$

The wave stress and current stress were represented as scalars with no direction, so they were combined to represent total stress (τ_{bTOTAL}) as

$$\tau_{bTOTAL} = \left(\tau_{bWAVE}^2 + \tau_{bCURRENT}^2\right)^{1/2} \quad (7)$$

following Wiberg and Smith (1983).

Suspended Sediment

Suspended sediment concentrations in the water column were calculated using the Rouse equation (Rouse 1937)

$$C_s = C_a\left[\frac{z(h - z_a)}{z_a(h - z)}\right]^{-\frac{w_s}{\kappa u_*}} \quad (8)$$

where C_s is suspended sediment concentration, C_a is a reference concentration at reference height z_a, z is height in the water column, w_s is particle settling velocity, u_* is shear velocity ($= \sqrt{\tau_b/\rho}$), and κ is von Karman's constant (0.41). The reference concentration (C_a) was calculated according to Smith and McLean (1977) as

$$C_a = C_{bed}\frac{\gamma S}{1 + \gamma S} \quad (9)$$

where $S = (\tau_b - \tau_{cr})/\tau_{cr}$ is the excess shear stress, C_{bed} is the bed concentration of the sediment, γ is a resuspension coefficient, and τ_{cr} is the critical shear stress for motion in the sediment bed. A value of 0.002 was used for γ in our model (Glenn and Grant 1987; Wiberg et al. 1994; Harris and Wiberg 1997) assuming a reference height of $z_a = 3D_{50}$, where D_{50} is the median grain size. This reference concentration was calculated using an excess shear stress based on $\tau_b = \tau_{bTOTAL}$, while the Rouse parameter in Eq. 8 ($-w_s/\kappa u_*$) was calculated using only the current shear velocity ($u_{*c} = \sqrt{\tau_{bCURRENT}/\rho}$). This approach reflects the ability of waves to suspend sediment only in a thin, near-bed wave boundary layer, while current shear velocities are required for mixing of sediment through the water column.

The maximum volume of sediment in suspension was limited to that present in a surface active layer. The thickness of the active layer (δ_{active}) was calculated using an expression developed for fine-grained sites on the California shelf (Harris and Wiberg 1997, 2001),

$$\delta_{active} = k_1(\tau_{bTOTAL} - \tau_{cr}) + k_2 D_{50} \quad (12)$$

with $k_1 = 0.007$ and $k_2 = 6$ for τ in Pascals and D_{50} in meters (Harris and Wiberg 1997). Because much of the sediment in this system is very fine and settles slowly, sediment that was suspended was allowed to remain in suspension until a deposition stress characterized by $u_{*c} = w_s$ was reached. The

sediment that was retained in suspension was included in determination of the volume of available sediment, so that the total volume of sediment actively suspended never exceeded the volume available in the active layer. Because the active layer was stress dependent, the amount of sediment retained in suspension was allowed to exceed the volume of sediment in the active layer.

The critical shear stress for sediment entrainment (τ_{cr}) was determined by examining the leading edge of suspension events, as recorded by the ADP, and observing the corresponding modeled shear stress. A critical shear stress of 0.04 Newtons m^{-2} determined in this way was used for the entire modeled area. This shear stress is lower than that predicted by the Shields curve for the average sediment size (Soulsby 1997), but is consistent with values from other studies of muddy sediments (e.g., Arfi et al. 1993; Lund-Hansen et al. 1999). The deposition stress, as well as suspended sediment concentrations, depends on particle settling velocity. Settling velocity was calculated for 11 size classes ranging from 1 to 750 μm using Stoke's Law for all sizes $<$ 100 μm and values from Dietrich (1982) for larger sizes. Flocculation, which is common in fine sediment suspensions in saline water (Eisma 1986; Hill 1998), increases the settling rate of the constituent grains. A floc sediment class with a settling velocity of 4.5×10^{-4} m s^{-1}, was created with half of the available $<$ 30-μm sediment. The settling velocity was determined by examining the end of sediment suspension events recorded by the ADP and the corresponding shear stresses. Published values of floc settling rates vary widely, but this value is within this range (e.g., Sternberg et al. 1999; Manning and Dyer 2002).

Results

Light Attenuation Equation

Based on a stepwise multiple linear regression, total suspended solids (TSS) was the only significant predictor of downwelling light attenuation (K_d), after correction for changes in path length caused by solar angle following Gordon (1989; m = 0.055, $r^2 = 0.93$, $p < 0.001$). Colinearity of POM and PIM prevented separation of the effects of these two constituents, so the total of the two, TSS, was used. For modeling light attenuation, coefficients from Gallegos (2001) were used to represent the concentration specific attenuation for chlorophyll (0.0154 m^2 (mg chl $a)^{-1}$) and dissolved organics (0.28 m^{-1} absorbance $units^{-1}$) because neither of these variables had significant relationships with light attenuation in Hog Island Bay. A value of 0.0384 m^{-1} was used for attenuation by seawater (Lorenzen 1972). To avoid overestimation of K_d because of inclusion of these values, measured values of K_d were recalculated as K_{dsed}, the light attenuation from suspended sediment, by subtraction of the K_{dwater} (from the water column), K_{dchla} (from chl *a*), and K_{d440} (from gilvin) from the measured K_d. K_{dwater} was determined based on the measurement depth of 1 m; K_{dchla} and K_{d440} were determined from measured values and the above concentration specific absorption coefficients. A new regression was calculated with TSS predicting K_{dsed}; the slope from this multiple regression ($m = 0.052$ m^2 g^{-1}, $r^2 = 0.91$, $p < 0.01$) was used to calculate attenuation from TSS. Light attenuation was then represented as

$$K_d(\mu_0) = \text{TSS} \times 0.052 + \text{chl a} \times 0.0154 + g_{440} \times 0.28 + 0.0384 \quad (13)$$

where μ_0 is the cosine of the solar zenith angle.

Chl *a* and g_{440} were retained in the equation to match standard practice, make the equation more applicable to other systems, and account for variability in pelagic primary productivity between the two modeled time periods. While chlorophyll and dissolved organics were not significantly correlated to light attenuation in Hog Island Bay, they have been found to significantly affect light attenuation in numerous other sites (e.g., Cerco and Cole 1993; Christian and Sheng 2003). Monthly averages calculated from a data set of monthly or bimonthly sampling at 10 sites in Hog Island Bay from July 1992 to February 1997 gave chl $a = 9$ and 2 μg l^{-1} for August and November, respectively. The average absorbance of 0.4 au at 440 nm for the 30 October 2003 data was used for g_{440} in both August and November (Gallegos 2001). Because values of both chlorophyll and g_{440} are low in this system, the inclusion of these two terms only results in a maximum increase in K_d of 0.24 m^{-1}. Calculated values of K_d were then used to estimate the percent light reaching the sediment surface following the Lambert-Beer law.

General Hydrodynamics

Astronomically-forced tidal flow was analyzed using results from the hydrodynamic model for the summer period, without any wind forcing. Hog Island Bay has semidiurnal tides with a phase lag of about 1.5 h from the inlet to the mainland. Depictions of the average relative velocities on ebb and flood tide showed lower velocities in shallow areas (0.05–0.1 m s^{-1} on the flats, 0.2–0.3 m s^{-1} in the channel) and farther from the inlet. Water entering and leaving the bay typically ran parallel to Machipongo Channel, unless it was diverted by shallow areas, such as the mid lagoon shoals on the east and west side of the channel and the two smaller islands to

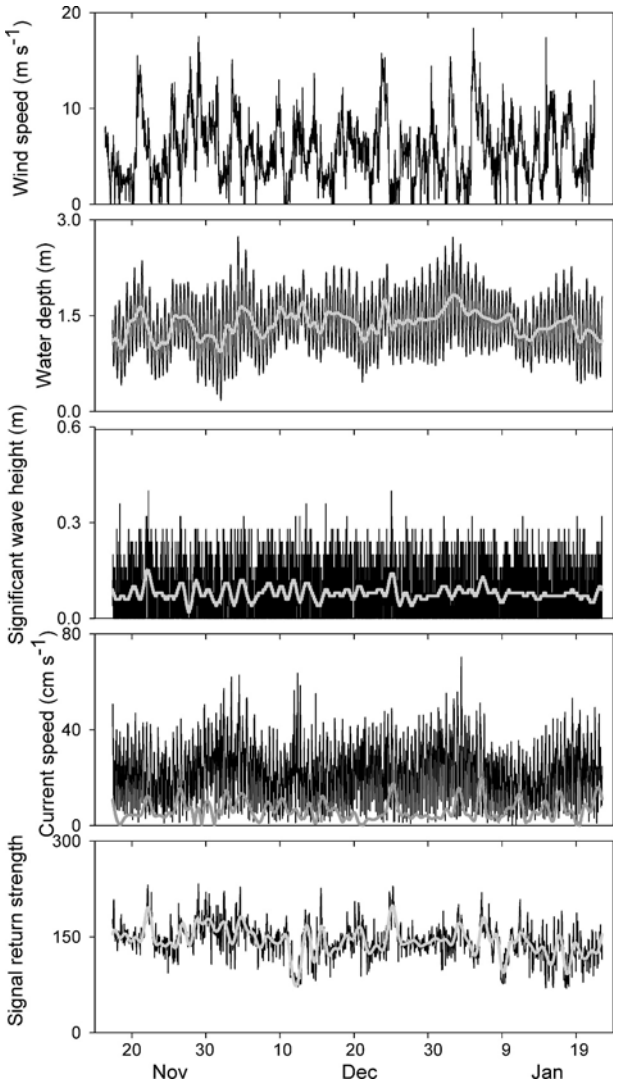

Fig. 2. Comparison of data measured on the ADP with wind data measured at Kiptopeke, Virginia. Black lines represent measured data; gray lines are the result of a low-pass filter. All variables show a response to increased wind speed, particularly on 11/21, 12/27, and 1/8. Signal strength is presented as a relative measure of suspended sediment concentration.

the west of Hog Island on the east side of the channel. Comparison of the summer wind and no wind model runs illustrates the effect of wind on currents. Wind effects were greatest in the shallow areas with a time averaged difference in velocity of 0.05–0.07 m s^{-1} on the shallow flats along the channel, roughly equal to the average velocity in this area.

The ADP data also showed that wind had a significant effect on currents. The velocities recorded by the ADP (Fig. 2) for ebb (mean = 0.251 m s^{-1}, maximum = 0.623 m s^{-1}) and flood (mean = 0.163 m s^{-1}, maximum = 0.433 m s^{-1}) tides showed ebb dominance (two-tailed *t*-test, $p < 0.001$, df = 3169). This asymmetry was largely due to wind effects. Filtering the time series to remove variations at frequencies lower than the tidal signal resulted in current velocities for ebb (mean = 0.202 m s^{-1}, maximum = 0.553 m s^{-1}) and flood (mean = 0.198 m s^{-1}, maximum = 0.548 m s^{-1}) tides that were not significantly different (two-tailed *t*-test, $p = 0.21$, df = 3169).

Wave heights in Hog Island Bay ranged from 0.00 to 0.53 m in the two modeled periods, with significantly higher waves with longer periods in late fall than in summer. Wave characteristics did not show much spatial variation across the bay. Seventy percent of the modeled area had an average significant wave height between 0.06–0.08 m in summer and 57% of the modeled area had an average significant wave height between 0.12–0.14 m in late fall. In summer, 87% of the modeled area had an average wave period of 0.6–0.8 s and 92% of the modeled area in late fall had an average wave period of 0.8–1.0 s.

Shear Stress

We characterized the spatial distribution of bed shear stresses in Hog Island Bay in terms of the shear stress one standard deviation (SD) above the temporal mean, reflecting the importance of high shear stress events for sediment suspension. Current bed stress during the summer and fall time periods was highest in the channel (> 0.08 N m^{-2}), coincident with the higher current velocities found there. Current stresses outside the channel were very low (0.00–0.02 N m^{-2}). Wave bed stress was minimal (0.00–0.02 N m^{-2}) in summer, but much higher on the shallow flats surrounding the channel in late fall (0.06–0.08 N m^{-2}). Total bed stress in Hog Island Bay was affected by both wave and current-generated stresses, particularly in the late fall when wave stresses were highest.

Sediment Suspension

The combination of waves and currents resulted in higher calculated values of TSS concentration in late fall than in summer. The temporal and spatial average of TSS for late fall was 48 mg l^{-1}, with minimum values behind the barrier islands and in the channel near the north end of the lagoon close to the mainland (Fig. 1). Maximum values were found on the northwest side of the marsh island near the northwest end of Hog Island, on the south side of the peninsula protruding into Hog Island Bay from the Delmarva Peninsula, and on the south and west side of the channel in the northern third of the lagoon. The temporal and spatial average of TSS in summer was 3 mg l^{-1} with little spatial variation outside the channel.

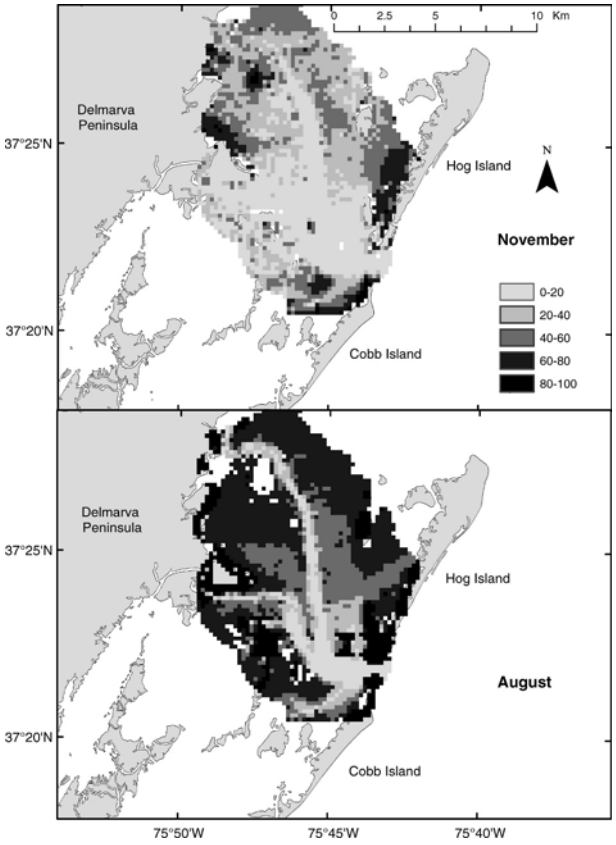

Fig. 3. Maps showing average percent light available for the August and November model periods. August shows light limitation only in the channel, while it is more widespread in November. For both time periods, the areas behind Hog and Cobb Islands receive the most light.

Light Availability

Light attenuation was greater in late fall than in summer (Fig. 3). In summer, the highest light attenuation was in the channel. While suspended sediment concentrations were higher in the channel, this greater light attenuation was largely due to the greater depth. In late fall, low light availability extended onto the flats near the channel, and light availability was highest in the sheltered areas behind the barrier islands where TSS was low. Average downwelling light available at the sediment surface was 55% in summer and 32% in late fall.

Model Validation

The modeling results of all components of the sediment transport model can be compared to the ADP data for model validation. The modeled current velocities (mean = 0.212 m s^{-1}, maximum = 0.487 m s^{-1}) at the ADP site agreed well with the measured depth-averaged velocity (mean = 0.220 m s^{-1}, maximum = 0.497 m s^{-1}, Fig. 4) during the period of the November model run (Fugate et al. 2006). The ADP recorded an average significant wave height (calculated as four times the standard deviation of the water elevation) of 0.08 m in the late fall. For the same time period, SWAN predicted an average significant wave height of 0.12 m at that location. The ADP only has a measurement accuracy of 0.01 m, resulting in measurement accuracy for significant wave height of 0.04 m.

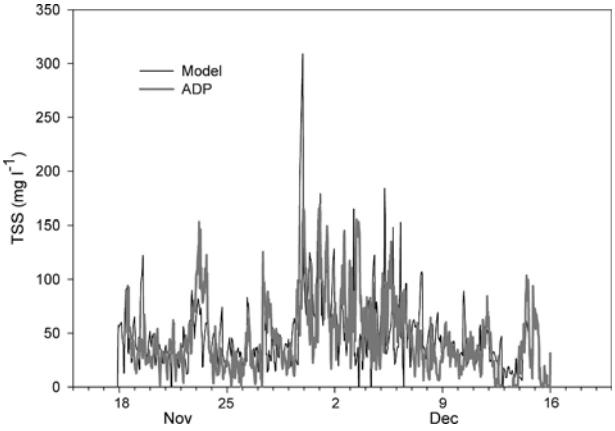

Fig. 4. Comparison of the modeled values for suspended sediment with measured values from the ADP for the November model period. The correlation coefficient between the two values is 0.41 ($p < 0.05$).

Modeled suspended sediment concentrations showed agreement with the ADP backscatter signal strength, and the corresponding values of TSS, derived from a calibration between ADP signal strength and TSS. The squared signal strength of the ADP backscatter was calibrated to TSS based on the April 2004 ADP deployment with a linear regression ($r^2 = 0.41$, $p < 0.01$, $n = 19$). This calibration was then applied to the November ADP data to calculate TSS, which were then resampled to match the timing of the model data. During the overlapping time period, the model predicted an average TSS concentration of 48 mg l^{-1} (SD = 34 mg l^{-1}) and the ADP measured an average TSS concentration of 51 mg l^{-1} (SD = 31 mg l^{-1}). The model results are correlated with the measured results with $r = 0.41$ ($p < 0.05$; Fig. 4). The correlation improves dramatically when measured and modeled values are binned by wind speed in 1 m s^{-1} increments ($r = 0.82$, $p < 0.01$; Fig. 5). In both the measured and modeled data, TSS was independent of wind at speeds less than 8 m s^{-1} (modeled: $r^2 = 0.04$, $p = 0.631$; measured: $r^2 = 0.02$, $p = 0.75$), but was directly related to wind speed at higher speeds (modeled: $r^2 = 0.83$, $p = 0.002$; measured: $r^2 = 0.77$, $p = 0.004$).

Surface water samples taken along two transects on 26 November 2002, one along the channel and

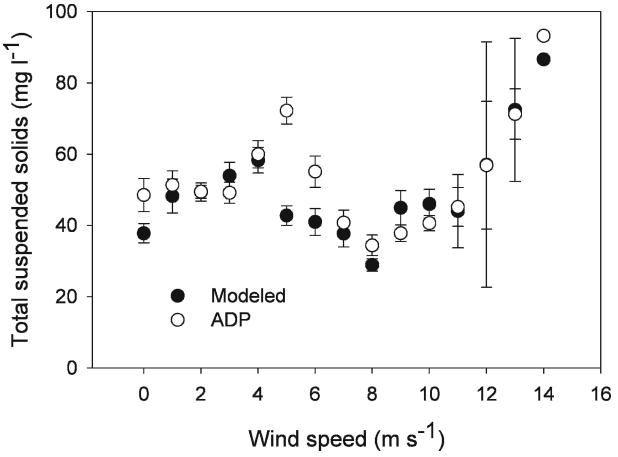

Fig. 5. Comparison of modeled and measured values of total suspended solids binned by wind speed. Modeled and measured values show good agreement and both show an increase in total suspended solids with increasing wind speed for wind speeds greater than 8 m s^{-1}.

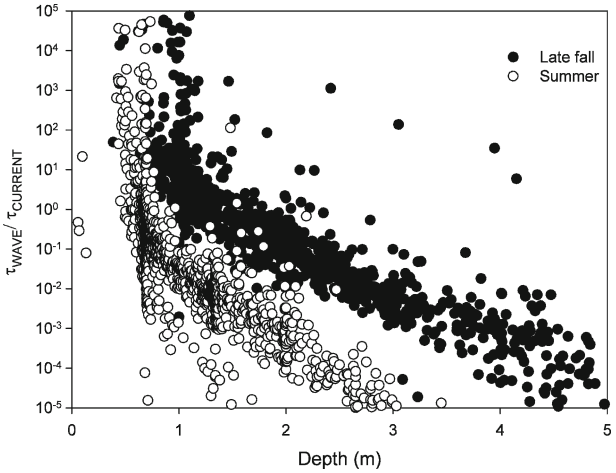

Fig. 6. The ratio of wave stress to tide stress is depth dependent, with wave stress increasingly important with shallow depths. The two model periods show different slopes because of the lower wind speeds in August.

the other across the channel, were compared to TSS predicted by the model. Samples from the across-channel transect of seven points had an average concentration of 26 mg l^{-1}, while the mean modeled value for the same transect was 18 mg l^{-1}. For the along channel transect, the average measured concentration (25 mg l^{-1}) was also similar to the modeled average concentration (18 mg l^{-1}). The model averages are both spatial and temporal averages, because all modeled values in the time period for the water sampling were averaged. In both cases the model slightly underestimates measured TSS, possibly because the averaging period includes a slack water period during which few water samples were taken.

Discussion

Suspended sediment clearly controls light availability in Hog Island Bay. The concentration of TSS was the only predictor of light attenuation based on a multiple stepwise linear regression. While the samples used to calculate this regression were from a single day during the fall, a time when primary productivity is likely low and sediment resuspension is likely high, the same trend can be expected year-round. The low pelagic primary productivity in most coastal lagoons (Sand-Jensen and Borum 1991) suggests that light attenuation will be controlled primarily by non-algal particulate matter. In a 2-yr study in Hog Island Bay, water column chlorophyll never exceeded 12 μg l^{-1} (McGlathery et al. 2001). Gallegos (1994) used an optical model to determine that in water bodies with chlorophyll concentration < 10 μg l^{-1} only a reduction in TSS can improve light availability. On the other hand, in systems with very low turbidity (< 1 NTU) only a reduction in chlorophyll can improve light availability. Christian and Sheng (2003) found that color (similar to g_{440} in this study) accounted for 5–25%, chlorophyll accounted for 10–26%, and non-algal particulate matter accounted for 59–78% of light attenuation in the Indian River Lagoon, with few measured values of chlorophyll over 10 μg l^{-1}. In highly eutrophic lagoons, such as the Maryland coastal bays, chl *a* concentrations can be as high as 45 μg l^{-1} and may be a more important predictor of light availability (Boynton et al. 1996).

Wind forcing is the dominant control on sediment suspension and consequently light attenuation, particularly in shallow areas of the lagoon. Most of the suspended solids in Hog Island Bay originate from internal resuspension. Hog Island Bay, like most coastal lagoons, does not have a significant freshwater source to deliver riverine material and erosion from the surrounding marshes likely only occurs during storm events (Christiansen et al. 2000). Spectral analysis of the ADP data for late fall-winter 2003 shows that while water velocity and depth both exhibited periodicity on tidal time scales (roughly 6 and 12 h), sediment suspension (measured as backscatter signal strength) showed no periodicity. This lack of a tidal signal indicates that sediment suspension was controlled by a non-periodic forcing, such as wind. The relative importance of currents and waves to suspended sediment concentrations is best described in terms of the shear stress they produce at the bed (Le Hir et al. 2000). The stress ratio ($\tau_{bWAVE}/\tau_{bCURRENT}$) was inversely related to depth (Fig. 6). A regression of

stress ratio and depth indicates that wave stress was dominant ($\tau_{bWAVE}/\tau_{bCURRENT} > 1$) for areas shallower than 1.6 m, or 60% of the modeled area, in November ($r^2 = 0.90$, $p < 0.001$, $n = 2444$) and for areas shallower than 0.6 m, or 24% of the modeled area, in August ($r^2 = 0.81$, $p < 0.001$, $n = 2423$). In both time periods, wave stress increased in importance as depth decreased. This trend is important in the context of light availability because shallow depths are more likely to be suitable habitat for submerged aquatic vegetation. Wind effects on currents were also highest in these shallow areas. The relationship between wind speed and light attenuation due to suspended sediment has been previously noted (e.g., Olesen 1996; Christian and Sheng 2003), but has rarely been addressed mechanistically.

The temporal and spatial variability shown in the modeling results indicates that this modeling approach is a better representation of light availability than other methods. Wind strongly influences light attenuation so fair weather monitoring will underestimate light attenuation. This approach also overcomes the limitations of strictly empirical models because it is based on physical process modeling. The model then requires less site calibration and should be applicable across a broader range of conditions. The initial work in creating and calibrating the model is extensive, but once this work is completed, the model can be used both to depict current conditions and to assess the effects of management decisions and climate change.

While this study supports the use of a sediment transport model to describe light availability, the model used here could be improved. This study used separate models to determine currents, both wind-driven and tidal, and waves and then combined the shear stresses generated by the hydrodynamics to determine sediment suspension. This combination of models is likely less accurate than a single unified model. The sediment suspension model used here did not include lateral transport of suspended sediment. In addition to improvements in basic modeling, this approach could also be improved by adding additional detail to the modeling. Light attenuation by suspended sediment is grain size dependent, with the higher surface area of finer sediment attenuating more light per unit mass (Baker and Lavelle 1984), meaning that a model maintaining separate size classes of suspended sediment could be more accurate. Light quality, the spectral characteristics of the available light, is important for primary producers and a wavelength specific model could be used to account for changes in light quality with attenuation.

The modeling approach presented here is being used to guide seagrass restoration efforts in Hog Island Bay following a 70-yr absence. Light availability has been identified as a dominant control on seagrass distribution (Gallegos and Kenworthy 1996; Moore and Wetzel 2000) and the increased turbidity that often follows a decline in rooted benthic macrophytes may decrease the area of available habitat. While estimates vary, seagrasses generally require 20% of incident radiation for growth (Duarte 1991). Based on the summer model results of average light availability, 88% of the sediment surface area is suitable seagrass habitat. Only 66% of the area is suitable habitat based on the late fall, windier modeling period. This difference represents 27 km^2 of seagrass habitat. The model is being used to select appropriate transplant sites increasing the probability for success of transplanted seagrasses. Recently, a naturally-occurring, recolonizing patch of seagrass was found just inland of Hog Island (Orth personal communication), in one of the locations deemed most suitable for seagrass growth during both modeling periods. Based on model results, this location received greater that 20% of incident radiation 90–100% of the time during both of the model periods. This area is characterized by relatively coarse sediments, likely in response to slightly elevated current stresses, and is sheltered by the islands leading to decreased wave stress. This type of location with sandy sediment and lower wave stress may be ideal for seagrass recolonization in coastal lagoons. One of the advantages of a physical modeling approach to light attenuation is the ability to not only identify suitable locations for restoration in one system, but also to illustrate general conditions that favor high light availability.

Acknowledgments

We would like to thank Joel Carr for his help with the SWAN modeling, the staff of the VCR/LTER for logistical support, and David New and Brenda Lam for field and lab help.

Literature Cited

Arfi, R., D. Guiral, and M. Bouvy. 1993. Wind induced resuspension in a shallow tropical lagoon. *Estuarine Coastal and Shelf Science* 36:587–604.

Baker, E. T. and J. W. Lavelle. 1984. The effect of particle size on the light attenuation coefficient of natural suspensions. *Journal of Geophysical Research* 89:8197–8203.

Betteridge, K. F. E., P. D. Thorne, and P. S. Bell. 2002. Assessment of acoustic coherent Doppler and cross-correlation techniques for measuring near-bed velocity and suspended sediment profiles in the marine environment. *Journal of Atmospheric and Oceanic Technology* 19:367–380.

Blom, G., E. H. S. Van Duin, R. H. Aalderink, L. Lijklema, and C. Toet. 1992. Modeling sediment transport in shallow lakes - Interactions between sediment transport and sediment composition. *Hydrobiologia* 235:153–166.

Blom, G., E. H. S. Van Duin, and L. Lijklema. 1994. Sediment resuspension and light conditions in some shallow Dutch lakes. *Water Science and Technology* 30:243–252.

BOOIJ, N., R. C. RIS, AND L. H. HOLTHUIJSEN. 1999. A third-generation wave model for coastal regions – 1. Model description and validation. *Journal of Geophysical Research* 104:7649–7666.

BOYNTON, W. R., I. MURRAY, J. D. HAGY, C. STOKES, AND W. M. KEMP. 1996. A comparative analysis of eutrophication patterns in a temperate coastal lagoon. *Estuaries* 19:408–421.

CERCO, C. F. AND T. COLE. 1993. 3-dimensional eutrophication model of Chesapeake Bay. *Journal of Environmental Engineering-ASCE* 119:1006–1025.

CERCO, C. F. AND T. M. COLE. 1994. Three-dimensional eutrophication model of Chesapeake Bay; Volume I, Main report. Technical report EL-94-4, U.S. Army Engineer Waterways Experiment Station, Vicksburg, Mississippi.

CHRISTIAN, D. AND Y. P. SHENG. 2003. Relative influence of various water quality parameters on light attenuation in Indian River Lagoon. *Estuarine Coastal and Shelf Science* 57:961–971.

CHRISTIANSEN, T., P. L. WIBERG, AND T. G. MILLIGAN. 2000. Flow and sediment transport on a tidal salt marsh surface. *Estuarine Coastal and Shelf Science* 50:315–331.

CLOERN, J. E. 2001. Our evolving conceptual model of the coastal eutrophication problem. *Marine Ecology Progress Series* 210:223–253.

DIETRICH, W. E. 1982. Settling velocity of natural particles. *Water Resources Research* 18:1615–1626.

DUARTE, C. M. 1991. Seagrass depth limits. *Aquatic Botany* 7:139–150.

EISMA, D. 1986. Flocculation and de-flocculation of suspended matter in estuaries. *Netherlands Journal of Sea Research* 20:183–199.

FUGATE, D. C., C. T. FRIEDRICHS, AND A. BILGILI. 2006. Estimation of residence time in a shallow back barrier lagoon, Hog Island Bay, Virginia, USA, p. 319–337. *In* M. Spaulding (ed.), Proceedings of the 9th International Conference on Estuarine and Coastal Modeling. ASCE, Reston, Virginia.

GALLEGOS, C. L. 1994. Refining habitat requirements of submersed aquatic vegetation - role of optical models. *Estuaries* 17: 187–199.

GALLEGOS, C. L. 2001. Calculating optical water quality targets to restore and protect submersed aquatic vegetation: Overcoming problems in partitioning the diffuse attenuation coefficient for photosynthetically active radiation. *Estuaries* 24:381–397.

GALLEGOS, C. L. AND W. J. KENWORTHY. 1996. Seagrass depth limits in the Indian River Lagoon (Florida, U.S.A.): Application of an optical water quality model. *Estuarine Coastal and Shelf Science* 42: 267–288.

GLENN, S. M. AND W. D. GRANT. 1987. A suspended sediment stratification correction for combined wave and current flows. *Journal of Geophysical Research-Oceans* 92:8244–8264.

GORDON, H. R. 1989. Can the Lambert-Beer law be applied to the diffuse attenuation coefficient of ocean water? *Limnology and Oceanography* 34:1389–1409.

HARRIS, C. K. AND P. L. WIBERG. 1997. Approaches to quantifying long-term continental shelf sediment transport with an example from the Northern California STRESS mid-shelf site. *Continental Shelf Research* 17:1389–1418.

HARRIS, C. K. AND P. L. WIBERG. 2001. A two-dimensional, time-dependent model of suspended sediment transport and bed reworking for continental shelves. *Computers and Geosciences* 27: 675–690.

HILL, P. S. 1998. Controls on floc size in the coastal ocean. *Oceanography* 11:13–18.

HOLDAWAY, G. P., P. D. THORNE, D. FLATT, S. E. JONES, AND D. PRANDLE. 1999. Comparison between ADCP and transmissometer measurements of suspended sediment concentration. *Continental Shelf Research* 19:421–441.

HORNBERGER, G. M., J. P. RAFFENSPERGER, P. L. WIBERG, AND K. ESHLEMAN. 1998. Elements of Physical Hydrology. Johns Hopkins Press, Baltimore, Maryland.

IP, J. T. C., D. R. LYNCH, AND C. T. FRIEDRICHS. 1998. Simulation of estuarine flooding and dewatering with application to Great Bay, New Hampshire. *Estuarine Coastal and Shelf Science* 47:119–141.

KENWORTHY, W. J. AND M. S. FONSECA. 1996. Light requirements of seagrasses *Halodule wrightii* and *Syringodium filiforme* derived from the relationship between diffuse light attenuation and maximum depth distribution. *Estuaries* 19:740–750.

LAWSON, S. E. 2004. Sediment suspension controls light availability in a shallow coastal lagoon. M.S. Thesis. University of Virginia, Charlottesville, Virginia.

LE HIR, P., W. ROBERTS, O. CAZAILLET, M. C. CHRISTIE, P. BASSOULLET, AND C. BACHER. 2000. Characterization of intertidal flat hydrodynamics. *Continental Shelf Research* 20:1433–1459.

LORENZEN, C. J. 1972. Extinction of light in the ocean by phytoplankton. *Journal Du Conseil* 34:262–267.

LUND-HANSEN, L. C., M. PETERSON, AND W. NURJAYA. 1999. Vertical sediment fluxes and wave-induced sediment resuspension in a shallow water coastal lagoon. *Estuaries* 22:39–46.

MANNING, A. J. AND K. R. DYER. 2002. The use of optics for the in situ determination of flocculated mud characteristics. *Journal of Optics A- Pure and Applied Optics* 4:S71–S81.

MCGLATHERY, K. J., I. C. ANDERSON, AND A. C. TYLER. 2001. Magnitude and variability of benthic and pelagic metabolism in a temperate coastal lagoon. *Marine Ecology Progress Series* 216:1–15.

MOORE, K. A. AND R. L. WETZEL. 2000. Seasonal variations in eelgrass (*Zostera marina* L.) responses to nutrient enrichment and reduced light availability in experimental ecosystems. *Journal of Experimental Marine Biology and Ecology* 244: 1–28.

OERTEL, G., C. R. CARLSON, AND K. OVERMAN. 2000. Hog Island Bay, Virginia Bathymetric Survey using Trimble DGPS and Innerspace Digital Fathometer. Available online: http://www.vcrlter.virginia.edu/~crc7m/hogbay/hogbay.html.

OERTEL, G. F. 2001. Hypsographic, hydro-hypsographic and hydrological analysis of coastal bay environments, Great Machipongo Bay. *Journal of Coastal Research* 17:775–783.

OLESEN, B. 1996. Regulation of light attenuation and eelgrass *Zostera marina* depth distribution in a Danish embayment. *Marine Ecology Progress Series* 134:187–194.

ORTH, R. J., M. L. LUCKENBACH, S. R. MARION, K. A. MOORE, AND D. J. WILCOX. 2006. Seagrass recovery in the Delmarva coastal bays. *Aquatic Botany* 84:26–36.

RIS, R. C., L. H. HOLTHUIJSEN, AND N. BOOIJ. 1999. A third-generation wave model for coastal regions - 2. Verification. *Journal of Geophysical Research – Oceans* 104:7667–7681.

ROUSE, H. 1937. Modern conceptions of the mechanics of fluid turbulence. Transactions of ASCE. Volume 102, Paper No. 1965. New York.

SAND-JENSEN, K. AND J. BORUM. 1991. Interactions among phytoplankton, periphyton, and macrophytes in temperate fresh-waters and estuaries. *Aquatic Botany* 41:137–175.

SMITH, J. D. AND S. R. MCLEAN. 1977. Spatially averaged flow over a wavy surface. *Journal of Geophysical Research* 82:1735–1746.

SOULSBY, R. L. 1997. Dynamics of Marine Sands. Thomas Telford, London, England.

STERNBERG, R. W., I. BERHANE, AND A. S. OGSTON. 1999. Measurement of size and settling velocity of suspended aggregates on the northern California continental shelf. *Marine Geology* 154:43–53.

VAN DUIN, E. H. S., G. BLOM, L. LIJKLEMA, AND M. J. M. SCHOLTEN. 1992. Aspects of modeling sediment transport and light conditions in Lake Marken. *Hydrobiologia* 235:167–176.

VAN DUIN, E. H. S., G. BLOM, F. J. LOS, R. MAFFIONE, R. ZIMMERMAN, C. F. CERCO, M. DORTCH, AND E. P. H. BEST. 2001. Modeling underwater light climate in relation to sedimentation, resuspension, water quality and autotrophic growth. *Hydrobiologia* 444:25–42.

WIBERG, P. AND J. D. SMITH. 1983. A comparison of field data and theoretical models for wave current interactions at the bed on the continental shelf. *Continental Shelf Research* 2:147–162.

WIBERG, P. L., D. E. DRAKE, AND D. A. CACCHIONE. 1994. Sediment resuspension and bed armoring during high bottom stress events on the northern California inner continental shelf - measurements and predictions. *Continental Shelf Research* 14: 1191–1219.

ZHAROVA, N., A. SFRISO, A. VOINOV, AND B. PAVONI. 2001. A simulation model for the annual fluctuation of *Zostera marina* biomass in the Venice lagoon. *Aquatic Botany* 70:135–150.

SOURCE OF UNPUBLISHED MATERIALS

ORTH, R. J. personal communication. Department of Biological Sciences, Virginia Institute of Marine Science, Gloucester Point, Virginia.

Received, October 5, 2005
Revised, July 6, 2006
Accepted, August 25, 2006